Geosynthetics, J. Kuwano & J. Koseki (eds)
© 2006 Millpress, Rotterdam, ISBN 90 5966 044 7

Model tests for new lightweight thrust restraint using geogrid

Kawabata, T., Sawada, Y., Uchida, K. & Kitano, T.
Faculty of Agriculture, Kobe University, 1-1, Rokkodai, Nada, 657-8501, Kobe, Japan

Ling, H.I.
Department of Civil Engineering, Columbia University, 120th Street, New York, NY 10027

Hirai, T.
Mitsui Chemicals Industrial Products, LTD, 3-39-10, Yushima, Bunkyo, 113-0034, Tokyo, Japan

Saito, K.
Development Section, Taisei Kiko Co., LTD, 14-5, Tekunopark, 669-1339, Sanda, Japan

Keywords: buried pipeline, thrust force, model test, geogrid, numeral analysis

ABSTRACT: Concrete blocks are commonly used at the bend of buried pipelines to restraint thrust force. However the heavy concrete blocks move significantly in earthquake or exhibit large settlement in soft ground. In this paper, the use of geogrid as thrust restraint was proposed and the lateral loading tests for this new light weight method was conducted using model pipe having a diameter of 90 mm in order to examine the effect and the resistant mechanism.

1 INTRODUCTION

Thrust force is generated at the bend of pipelines due to internal pressure. That moves the pipe bend to the backside. In current design, the concrete block is commonly installed at the bend to resist the thrust force.

Examinations on lateral loading for underground structures have been discussed from 1960s. Ovsen et al. (1964). In addition Rowe et al. estimated lateral ultimate capacity for anchor in sand by FEM. Furthermore in 1970's Akinmusuru (1978) and Audibert et al. (1977) investigated the behavior of lateral movement for anchor or buried pipe in dry sand. Trautmann et al. (1983) studied the behavior of movement in the lateral and vertical directions for buried pipe in dry sand and estimated the maximum resistance under different depth of cover. However, the distribution of earth pressure acting on underground structure was not mentioned in these studies.

Kawabata et al. (2002) conducted a series of lateral loading tests using a rigid pipe with 20 bi-axial load cells and the square piece. As a result, it was clear that due to the difference in friction between the pipe and backfills, earth pressure distribution changed remarkably and the horizontal penetrating resistance was approximately 60-70% in comparing with the square piece. In order to establish accurate design procedure it is indispensable that more experiments and numeral analysis need to be conducted.

Concrete blocks are effective in resisting lateral thrust force. However, according to the report on the damages of buried pipeline due to liquefaction (Mohri et al., 1997), heavy concrete blocks will be a weak point during earthquake due to its inertia force. Therefore lightweight thrust restraint is required.

In this paper, lightweight thrust restraint was proposed. The lateral loading tests for buried pipe were conducted using a model pipe having a diameter of 90 mm. Furthermore particle image velocimetry analysis (PIV) for model ground surface and numerical analysis by Distinct Element Method (DEM) is conducted to clarify the resistance mechanism.

2 OUTLINE OF TESTS

A medium size rigid steel test pit ($2.0 \times 0.5 \times 0.5$ m) was used in the experiments as shown in Figure 1. The model pipe having a diameter of 90 mm as shown in Figure 2 was used. Assuming concrete block, a square piece (90×90 mm) was also used. The depth of the cover H was 50, 100 and 150 mm. After backfilling, the buried pipe was loaded in the lateral direction at 0.5 mm/min using a jack.

The properties of the backfill sand are shown in Table 1. Density of sand was approximately D_r = 90%. Six types of model pipe were investigated as shown in Table 2. Note that a rigid plate was installed in order to unite soil mass wrapped by geogrid in

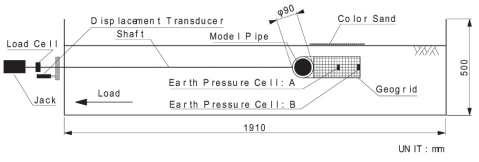

Figure 1. Cross section of test.

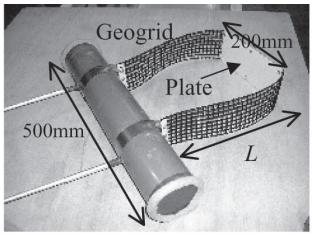

Figure 2. Model pipe (Type-5).

Table 1. Properties of backfill sand (Silica sand).

Density, ρ [g/cm^3]	2.641
Minimum dry density, ρ_{min} [g/cm^3]	1.232
Maximum dry density, ρ_{max} [g/cm^3]	1.575
Water content, ω [%]	0.018
Friction angle ϕ (degree)	39.8
Uniformity coefficient U_c	2.09

Table 2. Type of tests

Type_1	Model of blank pipe
Type_2	Model of concrete block
Type_3	2 sheets geogrid having length 300 mm
Type_4	2 sheets geogrid having length 450 mm
Type_5	Geogrid having length 300 mm with plate
Type_6	Acrylic having length 300 mm with plate

Type_5. In Type_6, acrylic was used to represents high strength geogrid.

The geogrid used in the tests was HDPE and the tensile strength was 3.5 kN/m. Figure 3 shows the relationships (σ_n-τ') from pull-out tests. In pull-out tests, anterior displacement and backside displacement were measured to evaluate the average tensile strain of geogrid. Figure 4 shows the relationships between pull-out ratio and average strain. Pull-out ratio is defined as percentage of anterior displacement over geogrid length.

3 RESULTS AND DISCUSSIONS OF EXPERIMENTS

3.1 *Lateral resistance*

Figure 5 shows the relationships between horizontal displacement and lateral resistance in Type_1-5 under H = 50 mm. Lateral resistance steadily is increasing with displacement. The maximum lateral resistance in Type_2 simulating concrete block is approximately 1.4 times that of Type_1. Resistance in all Types using geogrid are larger than that in Type_2. It is found that these new methods using geogrid were extremely effective as thrust restraint. Furthermore, in comparison the maximum resistance in Type_2 and 3, difference due to the length of geogrid is seen after 5 mm displacement. It can be considered that the resistance due to geogrid is seen for large deformation. In addition, by comparison

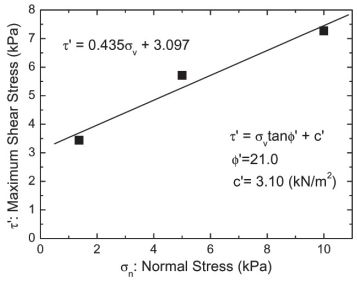

Figure 3. Relationship between normal stress and frictional resistance.

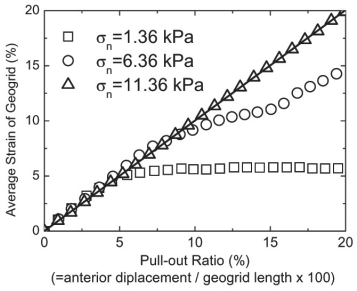

Figure 4. Relationship between pull-out ratio and average tensile strain.

the resistance in Type_3 and 5, the effect of rigid plate is seen slightly. However the difference appears after the peak of Type_3, it is considered that resistance due to plate was delayed due to extension of geogrid.

The relationships between lateral resistance and horizontal displacement in Type_5 and 6 under 50, 100 and 150 mm depth of cover condition are shown in Figure 6. Maximum resistance in both types increase with depth of cover. In addition, by comparing the resistance in Type_5 and 6, difference due to the strength of geogrid was not clearly seen. However it is thought that the effect of rigid plate of Type_6 is larger than that of Type_5 considering the fact that the frictional resistance between acrylic and sand is significantly small.

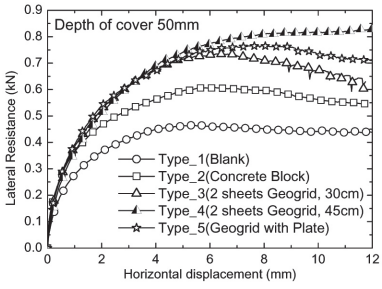

Figure 5. Relationship between displacement and resistance (H = 50 mm, Type_1-5).

© 2006 Millpress, Rotterdam, ISBN 90 5966 044 7

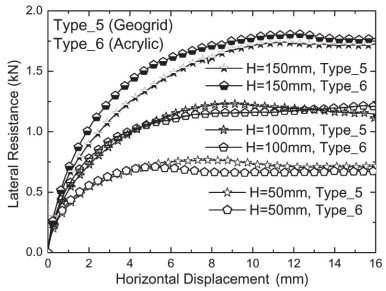

Figure 6. Relationship between displacement and resistance (H = 50, 100, 150 mm, Type_5 and 6).

3.2 *Earth pressure*

Horizontal earth pressure was measured to investigate the soil behavior between geogrid and in front of the plate as shown in Figure 1. Figure 7 shows the change of horizontal earth pressure A in Type_1-5 under 50 mm cover condition. Although horizontal earth pressure in Type_1 and 2 did not change, that in Type_3, 4, and 5 increase with the horizontal displacement. It is thought that soil between geogrid was compressed with displacement. Note that in Type_5 the earth pressure was more than 4 kPa. However the peak of the earth pressure in Type_5 is seen at around 10 mm, this result indicates that the factor of resistance was due to the stretching of geogrid.

Figure 8 shows the change of earth pressure B installed in front of the plate in Type_5 and 6. From

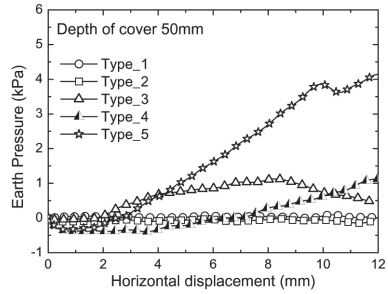

Figure 7. Changes of horizontal earth pressure A (H = 50 mm, type_1-5).

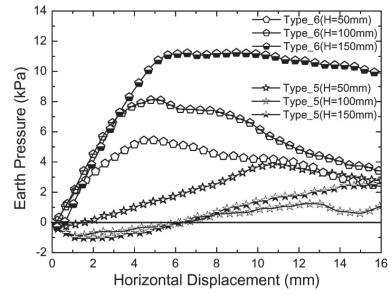

Figure 8. Changes of horizontal earth pressure B acting on the plate (H = 50, 100, 150 mm, Type_5 and 6).

Figure 8 it is understood that earth pressure in Type_6 has a peak around 5 mm displacement. On the other hand, in Type_5, it is not clear except depth cover of 50 mm. This behaviour is due to stretching of geogrid under large confining pressure as shown in Figure 4. Judging from these results, high strength geogrid is required if geogrid is buried deeply.

3.3 *Particle image velocimetry analysis*

In order to investigate the resistance mechanism due to the rigid plate, (Figure 1) color sand was equipped on the ground surface over the restraint and picture was taken with digital camera. In addition PIV analysis was conducted and ground displacement was shown by vectors.

Figures 9 and 10 show the results of PIV analysis for Type_5 and 6 at 4-8 mm horizontal displacement. From these results, it is seen that ground surface was moving in the same direction as the model pipe. In addition, it is easily found that soil outside restraint was moving. This soil behavior indicates a three-dimensional failure. By comparison Type_5 and 6, displacement in Type_5 was smaller than that in Type_6. It is considered that this difference was due to the strength of geogrid. Namely, as shown in Figure 7, earth pressure acting on the plate in Type_6 yielded at 4-8 mm displacement. On the other hand, that in Type_5 did not reach the peak.

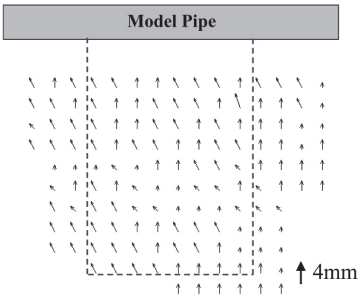

Figure 9. PIV analysis for Tyep_5 (From 4 to 8 mm horizontal displacement, H = 100 mm).

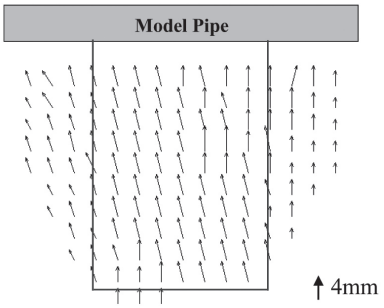

Figure 10. PIV analysis for Type_6 (From 4 to 8 mm horizontal displacement, H = 100 mm).

4 DEM ANALYSIS

In this paper, distinct element analysis (DEM) was carried out to examine the development of rupture surface in the sand ground for Type_6.

The parameters for the soil were; average particle size was 0.006 m, uniformity coefficient Uc was 1.52, rolling friction angle ϕ was 24 degrees, rolling friction coefficient was 1.0. The total particle numbers were about 25,000. The model pipe was a trussing polygon of 20 sides. Each element was connected by springs. The plate was modelled by beam element. The pipe were buried at depth of cover of 100 mm and were horizontally moved at a speed of 1.0 mm/s along with the plate. The analysis was conducted for Type_1 and Type_6. The results of analysis are shown in Figures 11 and 12.

The particles displacement at pipe displacement 4-8 mm is indicated by vector in Figures 11 and 12. From Figure 11, it is found that passive area developed in front of the pipe and active wedge formed in the back. On the other hand, in Type_6, the active wedge behind the pipe is not generated. In addition, the bottom plane between the pipe and the plate is mobilized. This behaviour is considered that stress behind the pipe is released and the soil mass compressed by the plate moves forward.

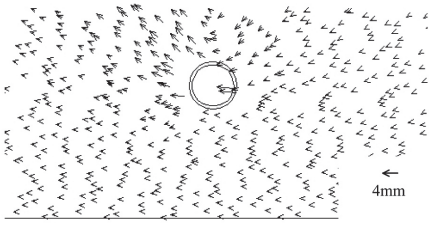

Figure 11. Particle displacement in Type_1 (From 4 to 8 mm horizontal displacement, H = 100 mm).

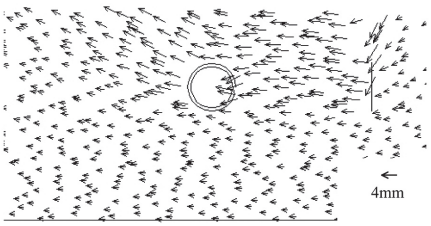

Figure 12. Particle displacement in Type_6 (From 4 to 8 mm horizontal displacement, H = 100 mm).

5 CONCLUSIONS

Lateral loading tests were conducted using the model pipe (ϕ = 90 mm) with geogrid as thrust restraint. Judging from the horizontal resistance and the horizontal earth pressure, it is found that the new method using geogrid is significantly effective method.

In addition, to investigate the resistance mechanism of the new method, PIV analysis for ground surface and DEM analysis in 2 D were carried out. As a result, it was found that the unification of soil between the model pipe and plate contributed to the resistance.

ACKNOWLEDGEMENTS

The DEM program used in this study was improved from “DEMS”. The authors gratefully acknowledge Prof. Sawada of Kyoto University for his assistance in this study. In addition, the advise by Dr. Nakase of Tokyo Electric Power Services Company on modelling DEM was greatly appreciated.

REFERENCES

Akinmusuru, J.O., Horizontally Loaded Vertical Plate Anchors in Sand, Journal of GT, ASCE, Vol. 104, GT2, pp. 283-286., 1978.

Audibert, J.M.E. and Nyman, K.J., Soil Restraint Against Horizontal Motion of pipes, Journal of GT, ASCE, Vol. 103, GT10, pp. 1119-1142, 1977.

Kawabata, T., Mohri, Y. and Ling, H.I., Earth Pressure Distribution for Buried Pipe Bend Subject to Internal Pressure, Proceedings of PIPELINES 2002, ASCE, Cleveland, Ohio, USA, CD, 2002.

Mohri, Y., Yasunaka, M. and Tani, S., Damage to Buried Pipeline Due to Liquefaction Induced Performance at the Ground by the Hokkaido-Nansei-Oki Earthquake in 1993, Proceedings of First International Conference on earthquake Geotechnical Engineering, IS-Tokyo, pp. 31-36, 1995.

Mohri, Y., Kawabata, T. and Ling, H.I., The Use of Geosynthetics in Mitigating Pipeline Flotation during Soil Liquefaction, Volume of Extended Abstracts of 10th International Conference on Soil Dynamics and Earthquake Engineering, Philadelphia, USA, p.135, 2001.

Ovesen, N.K., Anchor Slabs, Calculation Methods and Model Test, Bulletin 16, Danish Geotechnical Institute, Copenhagen, 1964.

Rowe, R.K. and Davis, E.H., The Behavior of Anchor Plates in Sand, Geotechnique, Vol. 32, No.1, pp. 25-41, 1982.

Trautmann, C.H. and O’Rourke, T.D., Behavior of Pipe in Dry Sand Under Lateral and Uplift Loading, Report to NSF, GT Eng. Report 83-7, 1983.

© 2006 Millpress, Rotterdam, ISBN 90 5966 044 7